Experimental analysis of thermal and damage evolutions of DCFC under static and fatigue loading

Jefri Bale [1], **Emmanuel Valot** [2], **Martine Monin** [3], **Olivier Polit** [2], **Claude Bathias** [2], **Tresna Soemardi** [4]

1. *Department of Mechanical Engineering, University of Nusa Cendana, Kupang-NTT, Indonesia*
2. *LEME - EA4416 - Univ. Paris Ouest - 50 rue de Sevres - 92410 Ville d'Avray - France*
3. *Department of Material Characterization and Validation, PSA Peugeot Citroën, Garenne Colombes (La), 92250, France*
4. *Laboratory of Mechanical & Biomechanical Design, Department of Mechanical Engineering, University of Indonesia, 16424 Depok, Indonesia*

ABSTRACT. *Discontinuous carbon fibre composite (DCFC) is a new low-cost material that has already been applied for commercial components, such as window frames of the Boeing 787 Dreamliner. Studying DCFC is very challenging because it does not show the same behaviour than conventional composites or isotropic materials. This work presents an experimental study of DCFC specimens submitted to static and fatigue tensile loading, based on mechanical and thermography non destructive evaluation (NDE) technique. An infra-red (IR) camera is used for real time monitoring of temperature change at the specimen outer surface. Under static loading, thermal response permits to well detect the early appearance of micro defects up to the final failure of DCFC material. Moreover, thermal response gives a good correlation with the damage evolution under fatigue loading. It is also shown that thermography method allows to successfully determine the high cycle fatigue strength (HCFS) of DCFC material.*

RÉSUMÉ. *Les composites à fibres de carbone discontinues (DCFC) sont des matériaux relativement récents qui ont déjà été employés pour la fabrication de composants industriels, tels que par exemple les contours de hublots des Boeing 787 Dreamliner. Cependant leur utilisation pour la réalisation de pièces structurelles reste encore marginale, leurs lois de comportement s'avérant être assez différentes de celles mieux connues des composites à fibres longues. Cette étude présente donc les résultats expérimentaux obtenus sur des éprouvettes trouées en DCFC soumises à des sollicitations de traction, en quasi-statique et en fatigue. Les éprouvettes sont équipées de jauges d'extensométrie et chaque essai est suivi par caméra infra-rouge (IR) afin de relever les variations de température apparaissant en surface d'éprouvette. Les essais quasi-statiques montrent que la caméra IR permet de relever, aussi bien de brèves variations de température localisées aléatoirement sur toute la surface de l'éprouvette dès les premiers niveaux*

Revue des composites et des matériaux avancés – n° 2/2016, 165-184

de chargements, quúne élévation de température progressive aux bords du trou à l'endroit où la rupture finale se produit. De plus, lors des essais de fatigue, il est montré qu'il existe une très bonne corrélation entre élévation de température et endommagement de l'éprouvette. Enfin, il est aussi montré que l'élévation de température de l'éprouvette est un paramètre qui permet de déterminer la limite de fatigue (HCFS) de ce matériau de manière beaucoup plus rapide que les méthodes traditionnellement employées.

KEYWORDS: *carbon fibre, discontinuous reinforcement, fatigue, thermal analysis.*

MOTS-CLÉS : *fibres de carbone, renforts discontinus, fatigue, analyse thermique.*

DOI:10.3166/RCMA.26.165-184 © 2016 Lavoisier

1. Introduction

Over the last decades, fibre-reinforced polymer composites have been used extensively in many applications of automotive and aerospace industry. Composites are known for their superior tensile strength, but they suffer poor resistance to impact and premature compression failure (Waas *et al*., 1998). In recent years, airframe manufacturers have proposed to use high-performance discontinuous composite systems which are suitable for compression moulding of primary structures (Harper, 2006). Discontinuous fibres are still predominantly used in non-structural elements, but over the last decade there has been significant progress for structural applications. Commercial applications for this type of material already exist: for instance, window frames of the Boeing 787 Dreamliner are made of a discontinuous carbon fibre composite (DCFC) (Porter, 2004). Several works (Harper, 2006; Boursier, 2001; Feraboli, Peitso, Cleveland, Stickler, Halpin, 2009; Qian *et al*., 2011; Bond *et al*., 2009; Feraboli *et al*., 2010; Feraboli, Peitso, Deleo *et al*., 2009; Feraboli, Peitso, Cleveland, 2009) have been conducted on fundamental studies concerning fabrication and mechanical properties of DCFC. Hexcel Corporation has developed a high performance discontinuous fibre compound that has been used for structural applications (Boursier, 2001). The increasing use of this material is driven by the fact that it allows compression moulding of complex parts at relatively low cost compared to continuous fibre composites. Nevertheless, regardless of how well a structural component is manufactured and maintained or how favourable the operating conditions are, many components can fail under fatigue loading. Composite materials exhibit very complex damage mechanisms under fatigue loading (matrix cracking, interfacial debonding, delamination, fibre rupture) because of anisotropic characteristics in their strength and stiffness (Bathias, 2006). Failure initiation theory developed by the industry for continuous fibre composite (CFC) can no longer be used to correctly describe this discontinuous fibre composite (DFC), because it does not behave like CFC or isotropic materials and defects affecting CFC do not affect DFC in the same way (Boursier, Lopez, 2010).

Many methods have been applied to observe damage mechanisms in composite materials, where the difficulty lies in the fact that damage is not visible to the naked

eye and can occur in many different forms. In order to enhance the safety of these composite structures, it is important to describe the appearance and growth of the damage under static and dynamic loads. In-service monitoring and diagnosis of complex structures requires the application of non-destructive and contactless methods. Non destructive evaluation (NDE) technique is a monitoring and observation method that is widely used in the composites field for assessing damage initiation and its growth until failure. It is advantageous to perform this inspection while the material is being tested, in order to save time and to remove the potential handling damage.

Thermography is a contactless NDE method which allows monitoring temperature changes at the specimen surface while test is achieved (Bayraktar *et al*., 2008). In addition this contactless method only needs a minimal surface preparation. Thermography investigation of composite materials has been already conducted in several studies (Muneer *et al*., 2009; Kutin *et al*., 2011; Colombo, Libonati, Pezzani *et al*., 2011; Libonati, 2010; Colombo, Libonati, Vergani, 2011). These show that thermography can efficiently identify the portion of surface that is subjected to stress and strain, and that it can successfully detect the damage propagation based on temperature changes. In case of polymer composites, a significant amount of heat, which is converted to a significant temperature increase, is generated by friction between fibre/fibre and fibre/matrix as well as by different damage mechanisms, such as fibre breaking, fibre-matrix debonding, matrix cracking, high viscoelastic matrix behaviour, etc. (Meneghetti *et al*., 2007; Steinberger *et al*., 2006; Soemardi *et al*., 1991). In this context, thermography is able to give valuable information on damage evolution during fatigue, which can be divided into three stages: (i) temperature varies due to frictions, (ii) temperature reaches a balance because of saturation in damage, (iii) an abrupt increase of temperature occurs at final rupture (Toubal *et al*., 2006). This third step gives the fatigue life of the specimen. In case of high cycle fatigue strength (HCFS) which is very time demanding, thermography-based approach has been extensively investigated (Curti *et al*., 1986; Toubal *et al*., 2005; Montesano *et al*., 2013). This approach, known as Risitano method (Curti *et al*., 1986), allows the HCFS determination for different composite materials (Toubal *et al*., 2005; Montesano *et al*., 2013). The main advantage of this method is to provide a rapid HCFS determination. Recently, Montesano et al. (Montesano *et al*., 2013) have developed this method for braided carbon fibre polymeric composite. Studies have already addressed the damage analysis of DCFC by NDE methods (Feraboli, Peitso, Cleveland, Stickler, Halpin, 2009; Qian *et al*., 2011; Bond *et al*., 2009), where a digital image correlation (DIC) has been used to monitor the full strain field of specimens with circular notch subjected to static tensile loading. When the hole is not large enough, results clearly show that high strain locations could occur far from the notch, which means that the presence of a small circular notch does not affect the DCFC specimen behaviour. The critical hole-to-width ratio threshold that ensures failure at the root of the notch for DCFC material has been found to be between 0.25 and 0.375 (Qian *et al*., 2011). Furthermore, (Feraboli *et al*., 2010) has studied defect and damage analysis of DCFC by ultrasonic inspection using pulse-echo C-scan ultrasound. In this work, initial real defects, such as macro voids, swirl or resin rich pockets, are found to have no correlation with fi-

nal failure position. For circular notch or open hole specimens, failure occurs away from the hole, and no direct relationship can be retrieved between this behaviour and the presence of significant signal attenuations during C-scan inspections. However, DCFC behaviour still remains fairly misunderstood.

The present study thus focuses on testing DCFC specimens under static and fatigue loads. Specimens are notched to ensure failure at the mid length. The damage behaviour is investigated by using thermography NDE technique, in order to obtain the HCFS of such a material. Then, Risitano method is used for DCFC material, and rapid analysis of fatigue strength is assessed. This analysis is achieved using correlation between ΔT increase and damage evolution for DCFC material. For this purpose, the paper is organized as follows. Section 2 describes experimental setup. Section 3 discusses successively the static, fatigue results and the rapid analysis of fatigue strength using thermal and damage evolution. Then, Section 4 draws final conclusions.

2. Experimental setup

The experimental study is divided into three stages: (i) tensile static test, (ii) tensile fatigue test, (iii) rapid thermography analysis to obtain the material HCFS. Surface of each specimen is observed by an infra-red (IR) camera during the entire test.

2.1. Materials

The material used is a discontinuous carbon fibre composite in chips or compounds form with 57% of nominal fibre volume and an epoxy matrix. Chip dimensions are $50\ mm$ length and $8\ mm$ width, which represents a good compromise between mechanical performance and manufacturing capability (Feraboli, Peitso, Deleo *et al.*, 2009).

Specimens have been cut from the same plate, and all have the same rectangular dimensions of $200\ mm$ length, $25\ mm$ width and $4\ mm$ thickness. A constant hole diameter of $10\ mm$ is afterwards machined at its centre. The hole diameter is equal to 0.4 width of the specimen, following (Qian *et al.*, 2011) recommendation. Glass/epoxy tabs of $50\ mm$ length are bonded at both ends of each specimen to ensure a good clamping during tests and to prevent premature failure in grips areas, see Fig. 1. Tabs are bonded using Redux 609 scotch weld film heated at $130°C$ for $30\ min$ to obtain optimum properties.

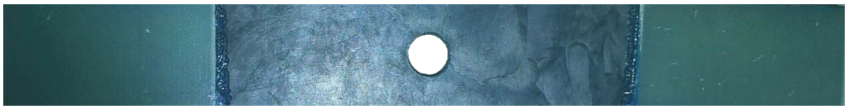

Figure 1. Example of DCFC specimen with an open hole and bounded tabs

2.2. Tensile test setup

Tests are carried out with an 8501 INSTRON Machine, equipped with hydraulic grips and a $100\ kN$ load cell. Static tensile tests are performed under a constant crosshead speed of $1\ mm/min$. The strain is measured using a single gage of $5\ mm$ length. Three specimens are tested under these conditions. Conversely, fatigue tests are performed under load control with a stress ratio $R = 0.1$, i.e. the $3\ Hz$ sinusoidal wave form loading has a minimum value ten times smaller than its maximum value. Strain, load and crosshead displacement are acquired with a frequency of $20\ Hz$ for all tests. The damage evolution is obtained using the global strain calculated from the crosshead displacement, as discussed in Section 3.1. One specimen is tested for each load case.

Two approaches can be used (Feraboli, Peitso, Cleveland, Stickler, Halpin, 2009) to calculate the strength of notched composite materials and are used in the following. The first one relies on the net strength, defined as:

$$\sigma_{HS} = \frac{P}{(w-d)\ t} \tag{1}$$

The second one neglects the presence of the hole and reads:

$$\sigma_{WHS} = \frac{P}{w\ t} \tag{2}$$

where P is the tensile loading, w is the specimen width, d is the hole diameter and t is the specimen thickness.

2.3. Thermography setup

A FLIR A325sc infrared (IR) camera is used to follow temperature changes on the specimen surface. Camera control and data recording are done with the FLIR R&D software which also allows an automatic calibration. Camera resolution is $320 \times 240\ pixels$ with an uncooled microbolometer detector. Camera spectral range is from 7.5 to $13\ \mu m$, whereas temperature range is from $-20°C$ to $120°C$ with an accuracy of $2°C$ or $2\ \%$ of reading. The IR camera is placed approximately $30\ cm$ away from the specimen surface in order to obtain full-field thermal maps. This thermography observation does not use an externally applied heat source (passive method). The thermal image acquisition is set at $30\ Hz$. Fig. 2 shows the experimental setup for the thermography measurement.

Results are given in terms of temperature variation $\Delta T = T - T_0$, where T is the surface temperature at time t and T_0 the initial surface temperature at $t = 0$. In addition the IR camera software optimizes the contrast between the region heating due to damage evolution and the adjacent undamaged region through a color scale.

Figure 2. Device setup used for both static and fatigue tests

3. Results and discussion

3.1. Static tensile test

A typical DCFC quasi-static tensile curve is shown in Fig. 3. This curve exhibits a non-linear behaviour with an ultimate tensile load of $28.2\ kN$, giving a $470\ MPa$ ultimate tensile strength (UTS) using Eq. (1) for a $1.7\ mm$ crosshead displacement. This DCFC specimen fails in a brittle mode, perpendicularly to the loading direction at the surface due to the first cracking, and in parallel to the thickness area because of subsequent delaminations, as seen in Fig. 4. Due to the hole size, failure always occurs close to the hole, at the specimen mid-length. Fig. 5 shows the stress-strain curve and local stiffness (LS) obtained from the $5\ mm$ uniaxial strain gages bounded at two different locations on the specimen surface.

Fig. 5 represents typical stress-strain curves in area with hole (gage 1 and Eq. (1)) and in area without hole (gage 2 and Eq. (2)) under the same tensile loading until failure. The presence of the hole reduces the cross-section and increases the calculated strength. These different stress-strain calculations yield to different LS measurements: $35290\ MPa$ for gage 1 and $46180\ MPa$ for gage 2.

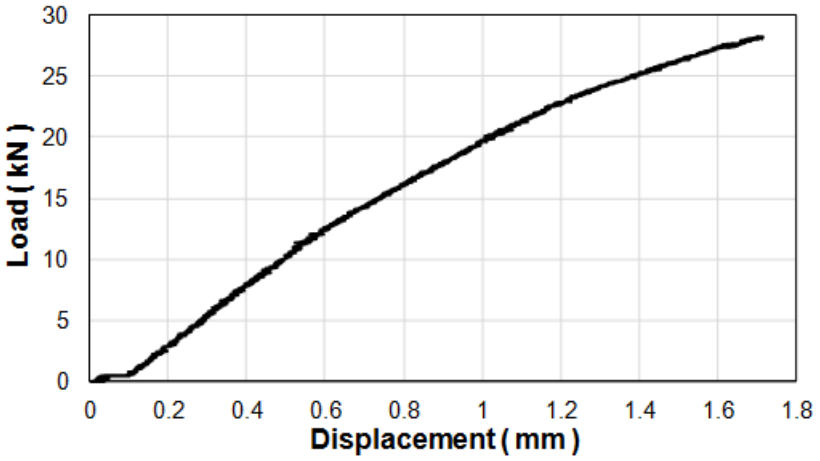

Figure 3. Typical static tensile curve for DCFC

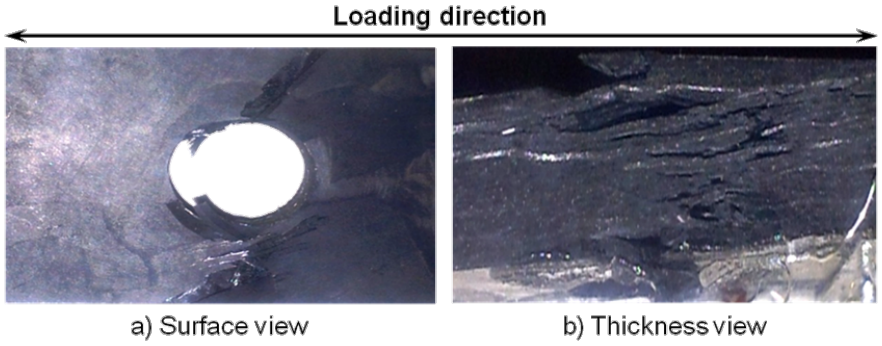

Figure 4. Catastrophic damage appearing when final failure arises

It should be noted that differences in stiffness measurements may also be originated by different local strain variations occurring at the surface of the DCFC material. Indeed, it appears that the specimen surface presents a highly non-homogeneous substructure derived from fabrication process using random compounds, which results in a heterogeneous strain distribution (Feraboli, Peitso, Cleveland, 2009).

3.2. Thermography observation of a static tensile test

Thermography images obtained by the IR camera during a tensile test are shown in Fig. 6. Before final failure, images show several very local peaks of ΔT, called

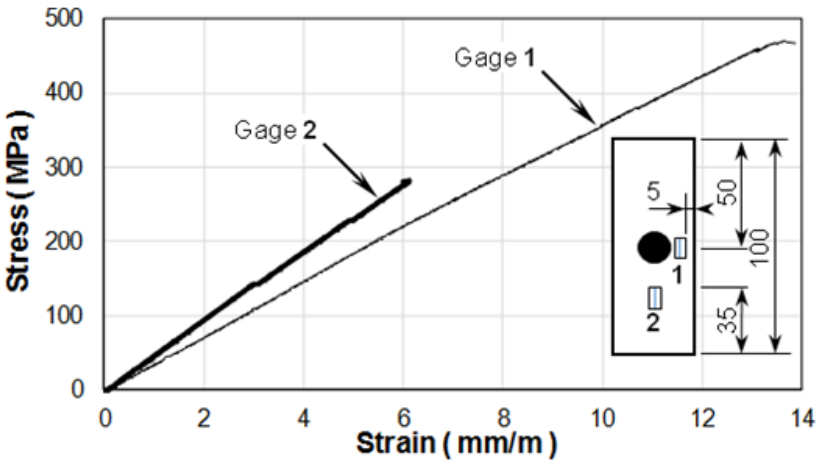

Figure 5. Stress-strain curves for DCFC subjected to a static test

hot-spots. These hot-spots, varying in location and intensity, are pointed out by black circles in Fig. 6. The central region of the specimen presents the higher temperature during the whole test, which increases until final failure.

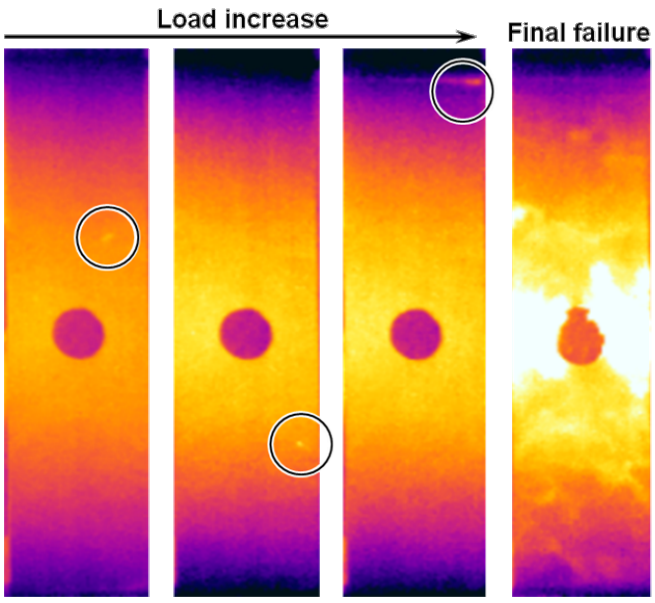

Figure 6. DCFC thermography images obtained during a static test

Temperature evolution appears according to two stages. In the first part, a minor increase of ΔT is recorded, which is possibly due to micro defect mechanisms appearing during the test. These micro defect mechanisms provoke some hot-spots that are visible by the IR camera only for a few seconds, and could be local debonding of compound tips from matrix. In the second part, a major increase of temperature is observed in a constant and large area where final failure eventually occurs. During this last stage, close to final failure, characteristic breaking sounds can also be heard.

In order to follow the ΔT evolution during the test, four subdomains defined on the specimen are shown in Fig. 7: one at each edge of the hole and the others closed to the clamps. Fig. 7 shows the ΔT evolution thereby obtained until final failure. Before final failure, the entire specimen surface presents a ΔT varying between 0.3 and $1.4^\circ\ C$. A ΔT above $0.7^\circ\ C$ is clearly shown by several hot-spots located close to the clamps as seen in Fig. 7a. When the final failure occurs, ΔT suddenly increases up to around $28^\circ\ C$ at the edge of the hole, as shown in Fig. 7b.

Considering the local ΔT evolution, it clearly appears that most of hot-spots do not indicate the final failure location. The presence of early hot-spots possibly brings out lower local mechanical properties coming from manufacturing defects or from the non-homogeneous chips nature. As a consequence, these early hot-spots seem to represent only sporadic local damages, which do not grow nor coalesce to form the macro damage. This phenomenon has already been pointed out by a previous study (Feraboli *et al.*, 2010). The final failure occurs at the edge of the hole which demonstrates that the hole diameter used for this study is large enough to produce such a stress concentration that the stresses in region away from the hole can be neglected. Thermography observation also confirms that all the micro defects giving early hot-spots have less effect than the hole triggering the critical damage. It is pointed out that this DCFC thermography behaviour is substantially different from that obtained for continuous fibre composite (CFC) where hot-spots often indicate the crack initiation or at least the location of macro defects. The sudden ΔT increase followed by final failure represents the energy which is released just before rupture. In areas with no macro damage, ΔT does not show any significant increase. Summarizing, we can conclude that minor ΔT increases are due to manufacturing defects while major ΔT increases are caused by macro defects related to significant macro damages.

3.3. Fatigue tensile test

For fatigue tests, specimens are subjected to a $3\ Hz$ sinusoidal loading. The maximum stress value attempted during this loading is defined in terms of a percentage of the UTS while the minimum stress value is taken to be 10% of the maximum stress value. UTS is obtained by averaging three quasi-static tensile test results. For each value of the normalized stress $\sigma_{max}/\sigma_{UTS}$, the number of cycles N_f at which the specimen fails is reported in the $S-N$ curve, as shown in Fig. 8, using only one specimen for each stress level. This $S-N$ curve is nearly linear and there is no failure after a run-off of $7.5\ 10^6$ cycles for a maximum stress level of 30% of UTS.

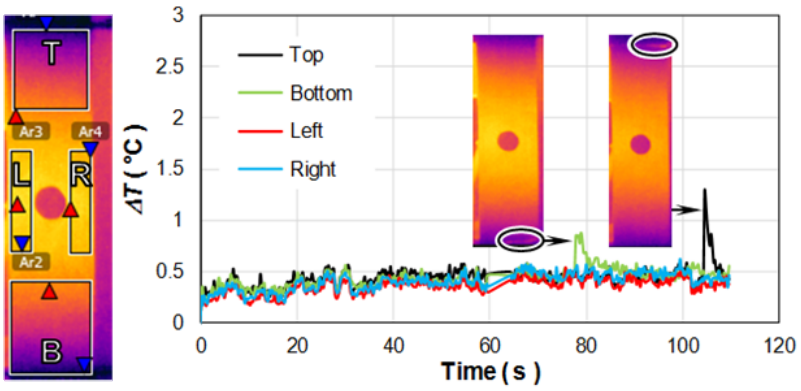

(a) Hot-spots at first stage of minor ΔT increases

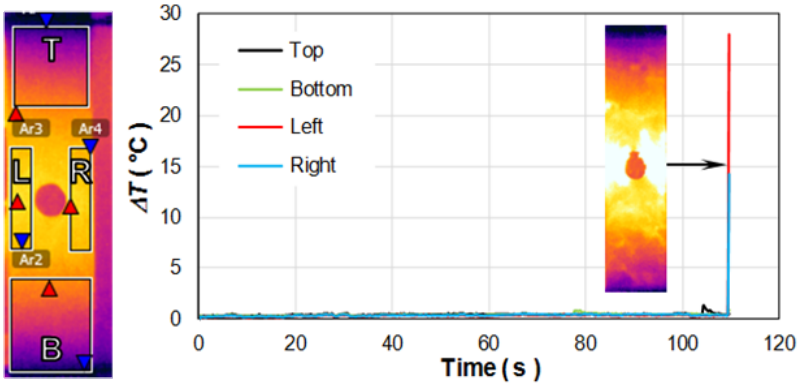

(b) Fixed heating areas as second stage of major ΔT increases

Figure 7. Evolution of the temperature variation ΔT during a static test

The S-N curve shows a gradual decline in fatigue strength when N_f increases. The trendline predicts a high cycle fatigue strength (HCFS) of about 0.43, that is to say that N_f reaches 10^6 cycles when the maximum stress value is around 43% of UTS. Hence for this DCFC material, a normalized stress level of up to about 0.43 (approximately $200\ MPa$) can be taken as a safe value for fatigue strength (i.e., the stress corresponding to a life of more than 10^6cycles).

The normalized S-N curve is then represented by Eq. (3) where the 0.05 value is called the fatigue sensitivity coefficient:

$$\frac{\sigma_{max}}{\sigma_{UTS}} = 1.23 - 0.05 \ln N_f \tag{3}$$

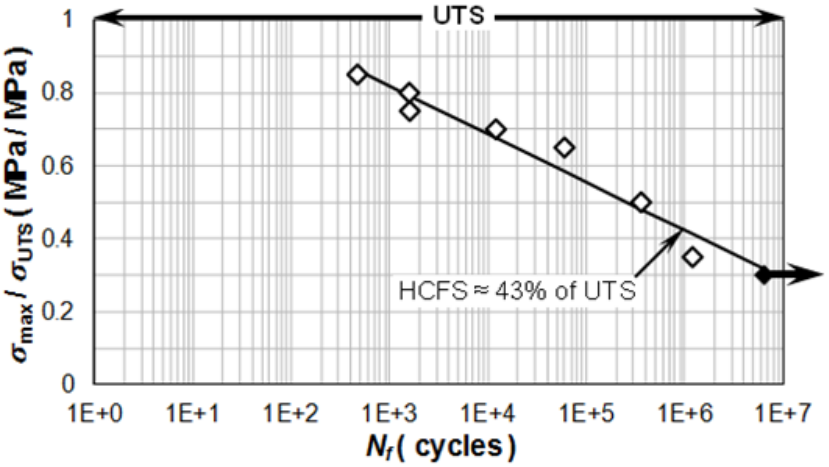

Figure 8. S-N curve obtained for DCFC

Two typical cumulative damage examples are given in Fig. 9. In these curves, D represents the cumulative damage defined as:

$$D = 1 - \frac{GS}{GS_0} \tag{4}$$

where GS and GS_0 are the global stiffness at any given loading cycle n and the initial global stiffness, respectively. In both examples D-curves show the same behavior: after an initial rapid increase (an average increase of about 10% during the first 20% of fatigue life), damage increases slowly until being close to the final failure; for the last 5% of fatigue life, damage increases suddenly and strongly as a consequence of the final catastrophic failure. In the present study, ΔT of the specimen subjected to fatigue loading is evaluated by an IR camera. Fig. 10 reports the average ΔT versus n for specimens loaded at different stress levels, using average value evaluated over the two regions at the hole edge (see Fig. 7) where the final failure takes place.

It can be seen that ΔT increases during fatigue testing for all the stress levels, but not in the same manner. ΔT response of the specimen loaded at 65% of UTS shows an increase during the first $n = 1000$ $cycles$. As the testing proceeds, however, ΔT remains nearly constant, with a rate of only $0.0002°$ $C/cycle$ until the end of the testing (12000 $cycles$). ΔT curve of the 70% shows a very similar trend in the initial loading phase as well as a very moderate increase of $0.005°$ $C/cycle$ until $n = 10500$ $cycles$, when an increase up to $\Delta T = 15°$ C is attained at a rate 10 times larger than in the preceding phase. The total failure is finally reached in only one cycle, and is accompanied by an abrupt increase of ΔT up to $37°$ C. The same 3 phases characterize the ΔT response of the 80% and 85% specimens. After a rapid increase of a few degrees at the beginning of the test, ΔT changes with a constant rate

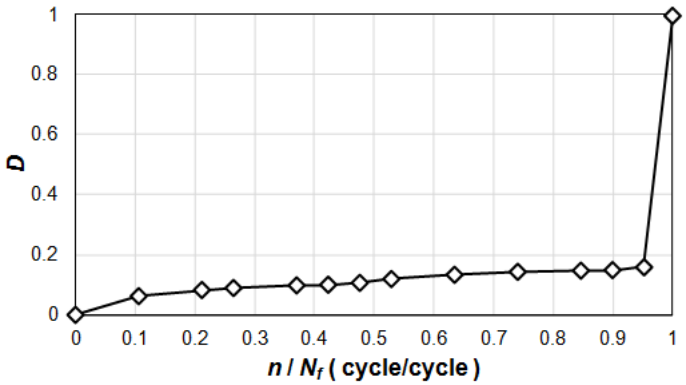

(a) Damage evolution for a load level of 80 % UTS ($N_f = 1580$ cycles)

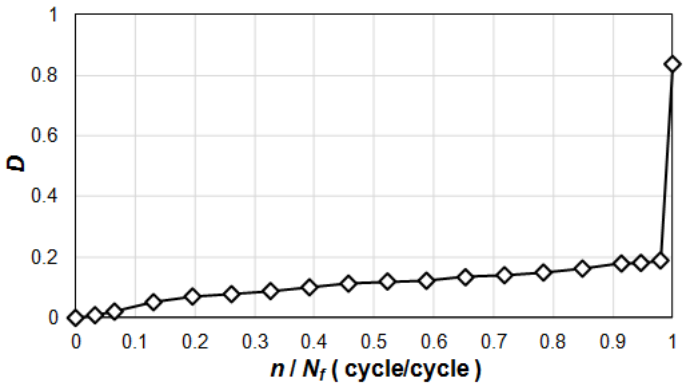

(b) Damage evolution for a load level of 85 % UTS ($N_f = 470$ cycles)

Figure 9. Typical damage evolution for DCFC specimens

(respectively $0.0066°\ C/cycle$ and $0.014°\ C/cycle$) until reaching the final failure, which is accompanied by an abrupt and very strong ΔT increase.

The hot zone, which localizes the damage area at the hole edge, is shown in Fig. 11 for the 80% specimen. Initial damage occurs at the hole edge (left image), and then propagates in the direction perpendicular to the loading (centre images) until reaching the final failure (right image). It can be noted that ΔT is not equal on both side of the hole, and this could be due to the material heterogeneity.

An evaluation of ΔT increase and damage evolution in DCFC material is now conducted. The superposition of ΔT and damage measurements obtained from global stiffness evolution (see Eq. (4)) are given in Fig. 12a for $80\ \%$ and in Fig. 12b for $85\ \%$ of UTS. The variation of the temperature ΔT with respect to damage D is presented in Fig. 13, indicating that ΔT and D are well correlated for this heterogeneous material.

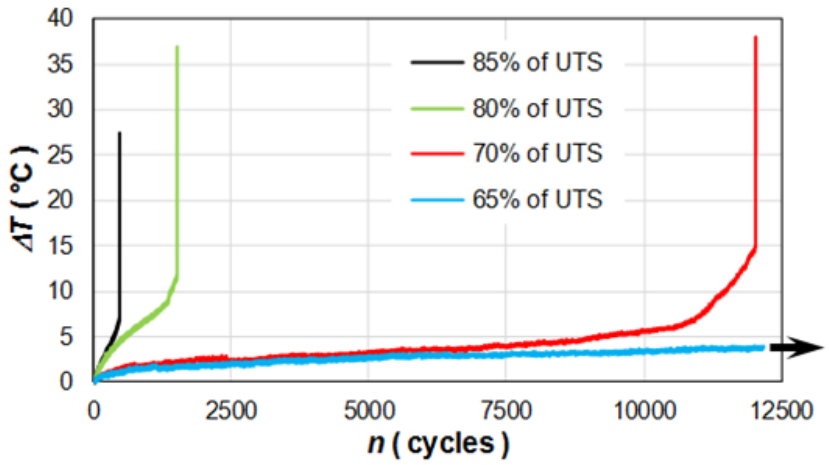

Figure 10. Temperature profile during fatigue test for different load levels

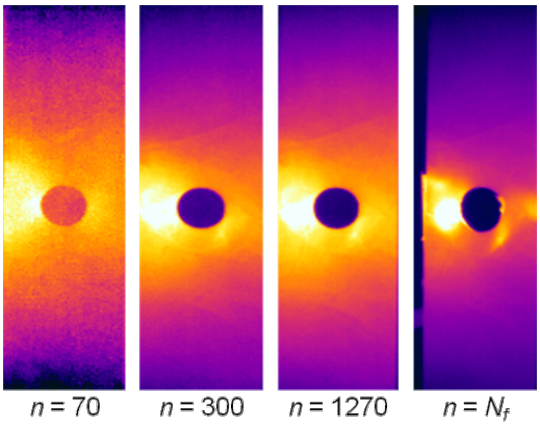

Figure 11. Thermography images at different cycle number for a load level of 80 % UTS

Therefore, it can be stated that the ΔT response can effectively estimate the damage behaviour of DCFC components subjected to fatigue loading.

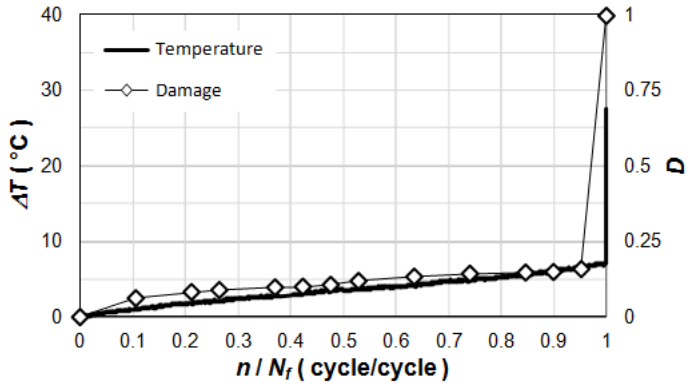

(a) Load level of 80 % UTS

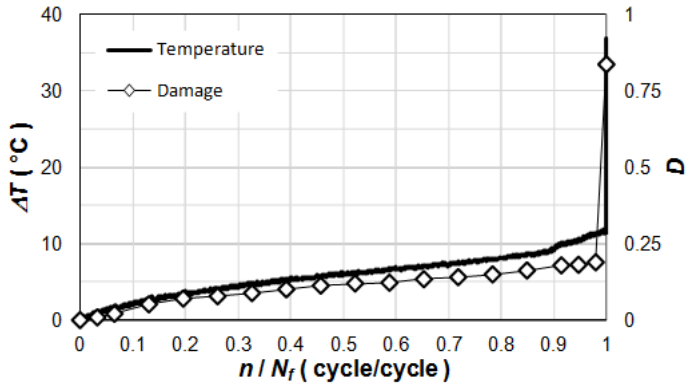

(b) Load level of 85 % UTS

Figure 12. Temperature and damage evolutions during a fatigue test for different load levels

3.4. Rapid analysis of fatigue strength based on thermography and energy dissipation

The purpose of this section is to assess Risitano method (Curti *et al.*, 1986) for DCFC material, combining thermography measurements and energy dissipation, as proposed in (Montesano *et al.*, 2013). The DCFC fatigue strength is evaluated on the basis of IR camera results and ΔT is recovered from the previous fatigue tests over several thousand of cycles which corresponds to approximatively 10^4 $cycles$ for each load level. The area around the hole is again used to trend the ΔT evolution and results are shown in Fig. 14. Using ΔT values coming from the stabilized part of the curve ($n = 6000$ is chosen), HCFS is then determined as the intersection of two

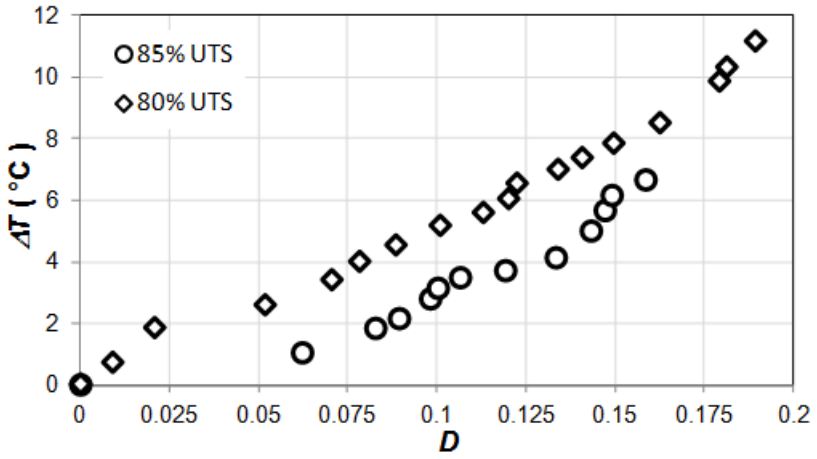

Figure 13. ΔT versus D for the two load levels

linear regressions that interpolate the ΔT_s for low and high load levels. The result of this procedure is shown in Fig. 15.

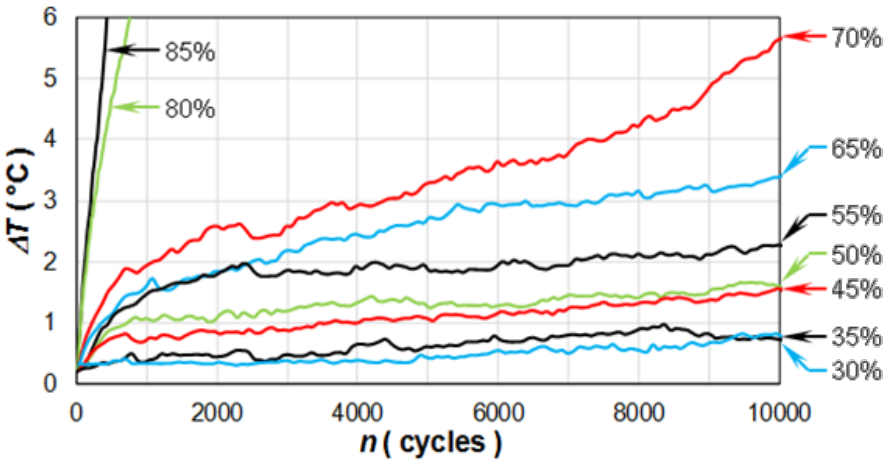

Figure 14. ΔT evolution obtained for each load level

An approach based on dissipated energy is next proposed in order to assess the thermography-base method for estimating HCFS. The energy dissipation per unit volume during one loading cycle is schematically shown in Fig. 16. The dissipated

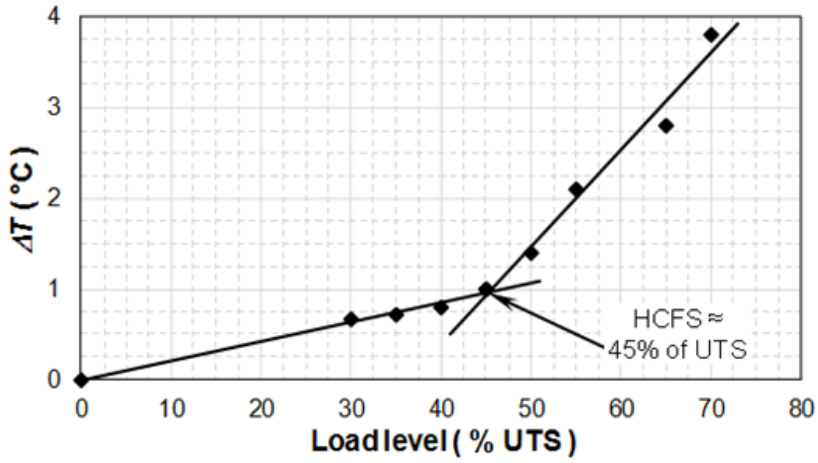

Figure 15. HCFS of DCFC determined by thermography approach

energy E_d is thus measured as the area of the hysteresis loop by the following equation:

$$E_d = \int_{\epsilon_{min}}^{\epsilon_{max}} \sigma_{load}(\epsilon)\, d\epsilon - \int_{\epsilon_{min}}^{\epsilon_{max}} \sigma_{unload}(\epsilon)\, d\epsilon \tag{5}$$

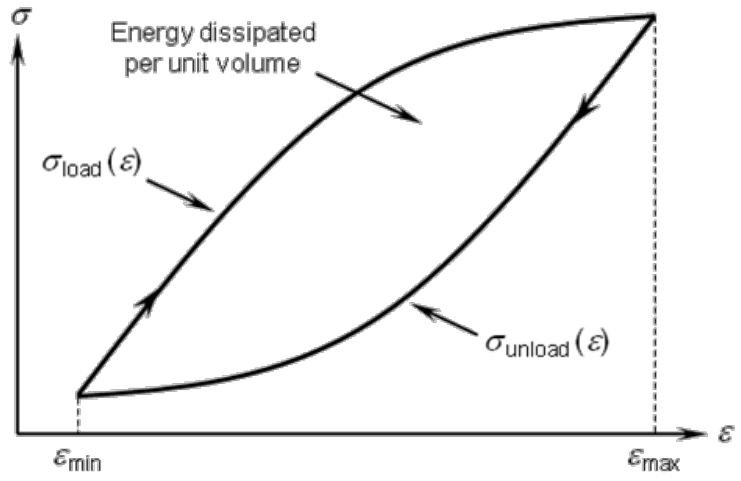

Figure 16. Schematic of quantifying dissipated energy E_d for any given cycle n

Fig. 17 gives an illustration of E_d evaluation for different load levels, while Fig. 18 shows a plot of E_d versus load level for the cycle $n = 6000$. Hence quite similar

HCFS values for DCFC are found with three different approaches: traditional Wöhler S-N curve (Fig. 8), direct thermography study (Fig. 15) or energy dissipation analysis (Fig. 17(b)).

Finally, relationship between ΔT_s and E_d is addressed. The data reported in Fig. 19 shows that a second order relation could be find between these two quantities. Therefore, the dissipated heat measured by the IR camera is in fact due to the intrinsic energy dissipation of the material, which is possibly caused by microscopic damage (Montesano *et al.*, 2013). As reported in (Meneghetti *et al.*, 2007; Steinberger *et al.*, 2006), the main mechanisms causing energy dissipation may be attributed to, among others, the viscoelastic nature of the matrix material, matrix cracking, fibre fracture, interface cracking/friction. In a DCFC material, the intrinsic energy dissipation can be produced by stress concentrations due to the heterogeneous substructures (components) and microscopic damage, such as chip cracking, matrix cracking and interface cracking between chip and matrix.

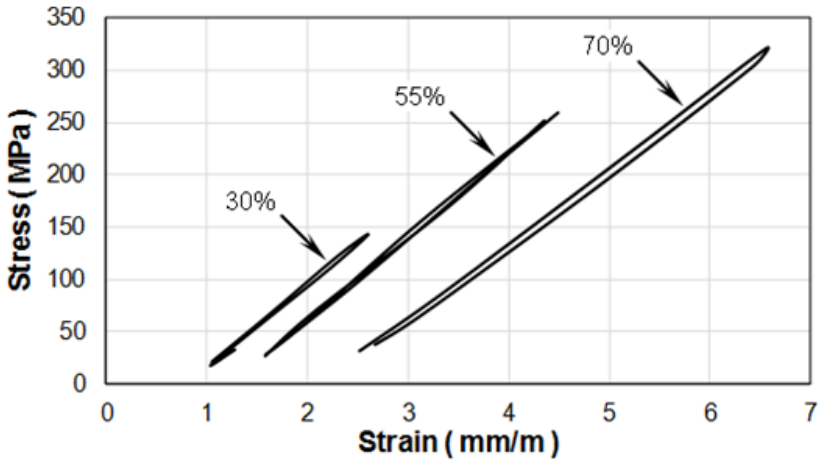

Figure 17. E_d calculation for different load levels with $n = 6000$ cycles

4. Conclusion

An investigation under both static and fatigue tensile loadings has been conducted on a DCFC material to have a better understanding of its damage evolution. Strain gages have been used to evaluate material local strains, and an IR camera has permitted to follow the temperature change during the entire test.

Under static loading, DCFC specimen exhibits high variation of local stiffness coming from fabrication process which uses random chip orientations. It is also found that IR thermography can be used to characterize damage growth on DCFC specimen. The micro defect, that can appear in the initial loading phase, is detected as a localized

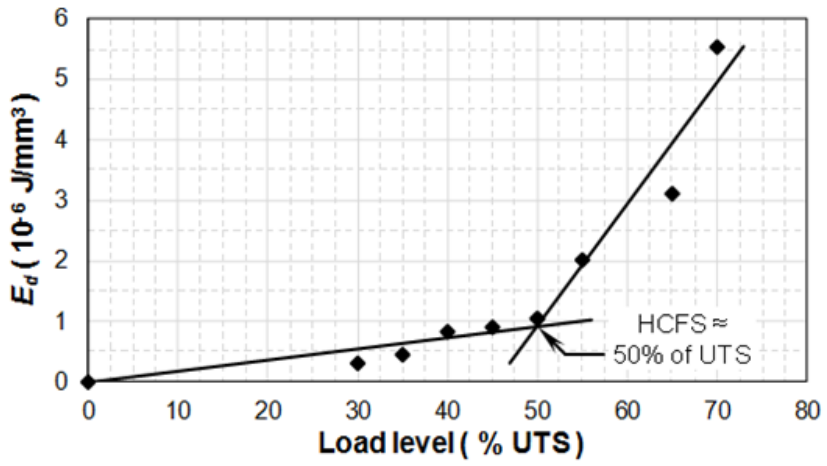

Figure 18. Bilinear approximation leading to the HCFS evaluation

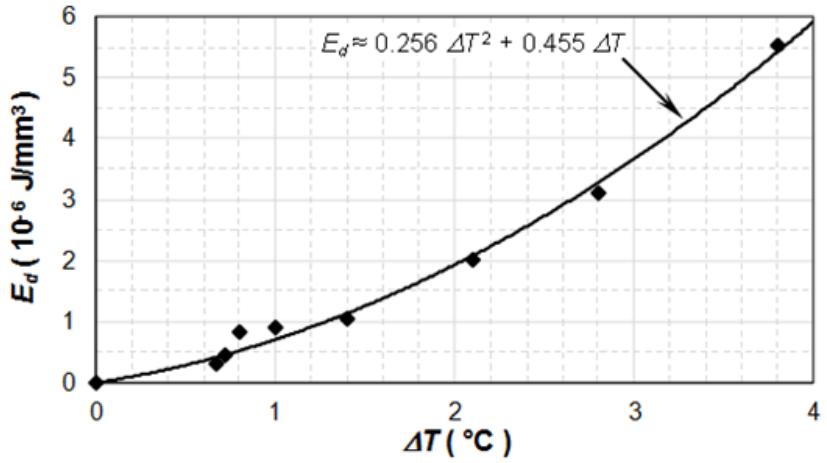

Figure 19. Evolution of the dissipated energy E_d versus intrinsic heating ΔT for DCFC

hot-spot by the camera. Each hot-spot may indicate manufacturing defect, and can occur anywhere in the specimen. On the contrary, the final DCFC failure is associated to a sudden temperature increase over a large area. The maximum temperature is then found at the final failure location.

Fatigue testing shows that thermal dissipation is related to the damage evolution of DCFC material. This work also shows that thermography and energy dissipation approaches can be successfully used to determine high cycle fatigue strength of DCFC material. The results found by these fairly quick approaches are in good accordance with those issued from the traditional Wöhler S-N curve, which is much more time consuming.

Acknowledgements

This work was funded by PSA Peugeot Citroën in France as a collaboration project with LEME laboratory of University of Paris Ouest Nanterre-La Défense. The Ministries of Education and Culture of Indonesia provided the financial support for the PhD studies of the first author.

References

Bathias C. (2006). An engineering point of view about fatigue of polymer matrix composite materials. *Int. J. Fatigue*, Vol. 28, pp. 1094–1099.

Bayraktar E., Antolovich S. D., Bathias C. (2008). New development in non-destructive controls of the composite materials and applications in manufacturing engineering. *J. Materials Processing Technology*, Vol. 206, pp. 30–44.

Bond M. D., Harper L. T., Turner T. A., Warrior N. A. (2009). Full - field strain measurement of notched discontinuous carbon fibre composites. In *Int. conf. composite materials (iccm17), edinburgh, uk.*

Boursier B. (2001). New possibilities with hexmc, a high performance moulding compound. In *22nd sampe european conference.*

Boursier B., Lopez A. (2010). Failure initiation and effect of defects in structural discontinuous fibre composites. In *Hexcel research and technology, 2010 (http://www.hexcel.com).*

Colombo C., Libonati F., Pezzani F., Salerno A., Vergani L. (2011). Fatigue behaviour of a gfrp laminate by thermographic measurements. *Procedia Engineering*, Vol. 10, pp. 3518–3527.

Colombo C., Libonati F., Vergani L. (2011). Study of the mechanical characteristics of gfrp by thermography. In *Int. conf. composite structures (iccs16).*

Curti G., La Rosa G., Orlando M., Risitano A. (1986). Analisi tramite infrarosso termico della 'temperatura limite' in prove di fatica (in italian). In *14th aias italian national conference*, pp. 211–220.

Feraboli P., Cleveland T., Ciccu M., Stickler P., DeOto L. (2010). Defect and damage analysis of advanced discontinuou carbon/epoxy composite materials. *Composite Part A*, Vol. 41, pp. 888–901.

Feraboli P., Peitso E., Cleveland T. (2009). Modulus measurement for prepeg-based discontinuous carbon fibre/epoxy systems. *J. Comp. Materials*, Vol. 43, No. 19, pp. 1947–1965.

Feraboli P., Peitso E., Cleveland T., Stickler P., Halpin C. J. (2009). Notched behaviour of prepeg-based discontinuous carbon fibre/epoxy systems. *Composite Part A*, Vol. 40, pp. 289–299.

Feraboli P., Peitso E., Deleo F., Cleveland T., Graves M., Stickler P. (2009). Characterization of prepeg-based discontinuous carbon fibre/epoxy systems. *J. Reinforcement Plastic Composite*, Vol. 28, pp. 1191–1214.

Harper L. T. (2006). *Discontinuous carbon fibre composite for automotive applications*. Unpublished doctoral dissertation, University of Nottingham.

Kutin M., Ristic S., Puharic M., Vilotijevic M., Krmar M. (2011). Thermographic testing of epoxy-glass composite tensile properties. *Contemporary Materials II*, pp. 88–93.

Libonati F. (2010). Damage analysis of composite by means of thermography. In *Symposium on experiment solid mechanics.*

Meneghetti G., Quaresimin M., De Monte M. (2007). Fatigue strength assessment of a short fibre-reinforced plastic based on the energy dissipation. In *Int. conf. composite materials (iccm16), kyoto, japan.*

Montesano J., Fawaz Z., Bougherara H. (2013). Use of infrared thermography to investigate the fatigue behaviour of a carbon fibre reinforced polymer composite. *Compos. Struct.*, Vol. 97, pp. 76–83.

Muneer K. M. M., Prakash R. V., Balasubramaniam K. (2009). Thermomechanical studies in glass/epoxy composite specimen during tensile loading. *Engineering & Technology*, Vol. 56, pp. 865–872.

Porter J. (2004). Moving closer to the goal of cost effective complex geometry carbon composite parts. In *19th asc technical conference, atlanta, usa.*

Qian C., Harper L. T., Turner T. A., Warrior N. A. (2011). Notched behaviour of discontinuous carbon fibre composites: Comparison with quasi-isotropic non-crimp fabric. *Composite Part A*, Vol. 42, pp. 293–302.

Soemardi T. P., Lai D., Bathias C. (1991). Static and fatigue biaxial testing of fibre composite using thin walled tubular specimens. Springer Verlag (Germany).

Steinberger R., Valadas Leitao T., Ladstatter E., Pinter G., Billinger W., Lang R. (2006). Infrared thermographic techniques for non-destructive damage characterization of carbon fibre reinforced polymers during tensile fatigue testing. *Int. J. Fatigue*, Vol. 28, No. 10, pp. 1340–1347.

Toubal L., Karama M., Lorrain B. (2006). Damage evolution and infrared thermography in woven composite laminates under fatigue loading. *Int. J. Fatigue*, Vol. 28, pp. 1867–1872.

Toubal L., Lorrain B., Peyruseigt F., Karama M. (2005). Détermination de la limite d'endurance d'un carbone/époxy par analyse thermographique (in french). In *17ieme congrès français de mécanique.*

Waas A. M., Hyun A. J., Khamseh A. R. (1998). Compressive failure of notched uniply composite laminates. *Composite Part B*, Vol. 29b, pp. 75–80.